to itself than to the halochromate. This also means that complex metal anions in general will be insulated to some extent from hydrolysis and other solvent-related reactions because there will be a paucity of free water molecules in their immediate vicinity.

Acknowledgment. The technical assistance of Rissel Tauber is gratefully acknowledged. We thank Dr. F. Eirich of the Polytechnic Institute of New York for his gift of poly(vinylpyridinium bromide).

Registry No. $TcCl_6^{2-}$, 16972-03-5; $TcBr_6^{2-}$, 19443-24-4; CrO_3Cl^-, 15906-70-4; $FeCl_4^-$, 14946-92-0; choline chloride, 67-48-1; tetra-*n*-butylammonium chloride, 1112-67-0; tetra-*n*-pentylammonium chloride, 4965-17-7; poly(vinylpyridinium bromide), 32492-40-3; cetyltrimethylammonium bromide, 57-09-0.

Contribution from the Inorganic Chemistry Laboratory, Oxford University, Oxford OX1 3QR, England, and Chemical Crystallography Laboratory, Oxford University, Oxford OX1 3PD, England

Crystal Structures of Mixed-Valency and Mixed-Metal Salts $A_2M^{III}_{0.5}Sb^{V}_{0.5}X_6$ (A = Rb, Cs; M = Sb, Bi, In, Tl, Fe, Rh; X = Cl, Br). A Powder Neutron Diffraction Study

KOSMAS PRASSIDES,* PETER DAY,* and ANTHONY K. CHEETHAM

Received June 15, 1984

The crystal structures of 11 mixed-valency and mixed-metal salts $A_2M^{III}_{0.5}Sb^{V}_{0.5}X_6$ (A = Rb, Cs; M = Sb, Bi, In, Tl, Fe, Rh; X = Cl, Br) have been determined by powder neutron diffraction at 4.7 K and in several cases also at 298 and 423 K. Structures were refined by the Rietveld method. In five cases (A = Cs; M = Sb, Bi, Tl; X = Cl and A = Rb, Cs; M = Sb; X = Br), superlattice ordering of SbX_6^- and MX_6^{3-} was found (space group $I4_1/amd$) while the remainder were disordered (space group $Fm3m$). The presence of order or disorder correlates with the average $M^{III,V}$–X bond length. In $Rb_2Sb^{III}_{0.5}Sb^{V}_{0.5}Br_6$, the $SbBr_6^{n-}$ groups are also tilted from the 4-fold axis at 4.7 K (space group $I4_1/a$). $Cs_2Sb^{III}_{0.5}Sb^{V}_{0.5}Cl_6$ retains distinguishable $SbCl_6^-$ and $SbCl_6^{3-}$ up to 423 K. Other physical properties (vibrational spectra) are discussed in the light of the structural results.

Introduction

The hexahalogenoantimonate(III,V) salts $A_2Sb^{III}_{0.5}Sb^{V}_{0.5}X_6$ have long been recognized as prototypes of Robin–Day[1] class II mixed-valency behavior, and their structural simplicity makes them ideal starting models for an understanding of the dynamics of intervalence electron transfer in weak interaction systems. Surprisingly, their structures have presented a longstanding puzzle. Early X-ray powder diffraction work[2] indicated that the salts crystallize with a structure isomorphous with that of K_2PtCl_6 (space group $Fm3m$), leading to the conclusion that the $Sb^VX_6^-$ and $Sb^{III}X_6^{3-}$ units are either crystallographically equivalent or randomly distributed. Later, X-ray single-crystal diffraction[3,4] established the presence of a superlattice in A_2SbBr_6 (A = NH_4, Rb).

To evaluate physical properties of these mixed-valency compounds, it is essential to have precise structural information, e.g. the difference in site geometry and bond length around the ions of differing oxidation states. In the case of the hexahalogenoantimonates(III,V), there have been reports that electron transfer may be sufficiently fast at high temperature to make the Sb sites equivalent on the Mössbauer time scale. In additon, with increasing temperature, the Sb^{III}–Cl stretching mode becomes weaker, suggesting that the oxidation state may lose its discrete character as phonons are progressively excited.

Given that the X-ray scattering in Cs_2SbCl_6 and related chlorides is dominated by the heavy elements Cs and Sb, we have undertaken a detailed investigation of the structural properties of the hexahalogenoantimonates(III,V) and mixed-metal salts with general formula $A_2M^{III}_{0.5}Sb^{V}_{0.5}X_6$ (A = Rb, Cs; M = Sb, Bi, In, Tl, Fe, Rh; X = Cl, Br) by powder neutron diffraction at temperatures from 4.7 to 423 K. A preliminary report of some of our results has appeared elsewhere.[5]

Experimental Section

All the compounds were prepared by standard methods[6,7] from HCl (or HBr) solutions of the constituent ions. X-ray powder diffraction was employed to ensure their purity. In order to suppress debromination, Rb_2SbBr_6 and Cs_2SbBr_6 were sealed in a tube under a bromine atmosphere. The powder neutron diffraction data were obtained on the high-resolution powder diffractometer, D1A, at the Institut Laue-Langevin, Grenoble, using neutrons with a mean wavelength of 1.909 Å. The samples were mounted in vanadium cans placed in a standard liquid-helium cryostat or an evacuable furnace. Diffraction data were collected in steps of 0.05°. The raw data from the 10 counters were merged by using Hewat's computer program.[8] After background subtraction, profile refinements were performed by using either the POWDER system[9] on the SERC Interactive Computing Facility or the modified version of the Rietveld program[10] on the Oxford University ICL 2988 computer. Neutron scattering lengths were taken from Bacon.[11] Since chlorine has a large mass absorption coefficient, an absorption correction was applied to the thermal parameters. An "effective" overall temperature factor due to absorption was calculated[12] and kept fixed during refinement while the individual isotropic temperature factors of all the atoms were refined independently.

Results

Cubic Salts. The simplest powder neutron diffraction profiles were obtained from the compounds $Rb_2M^{III}_{0.5}Sb^{V}_{0.5}Cl_6$ (M = Tl, In, Fe, Rh) and $Cs_2M^{III}_{0.5}Sb^{V}_{0.5}Cl_6$ (M = In, Fe) at 4.7 K. The small number of very sharp peaks indicates the high symmetry of the structure. Further, the background was flat and the signal-to-noise ratio excellent. A systematic investigation near the background level confirmed the absence of weak superlattice peaks, and all the reflections present in the profiles can be accounted for by the space group $Fm3m$. The difference between the $A_2M^{III}_{0.5}Sb^{V}_{0.5}Cl_6$ salts and the $A_2M^{IV}Cl_6$ antifluorite crystals is that the former contain two different octahedral units MCl_6^{3-} and $SbCl_6^-$ with M^{III} and Sb^V having different neutron scattering lengths, *b*. To perform the Rietveld refinement,[10] a random

* To whom correspondence should be addressed at the Inorganic Chemistry Laboratory.

(1) Robin, M. B.; Day, P. *Adv. Inorg. Chem. Radiochem.* **1967**, *10*, 248.
(2) Jensen, K. A. *Z. Anorg. Allg. Chem.* **1937**, *232*, 193.
(3) Lawton, S. L.; Jacobson, R. A. *Inorg. Chem.* **1966**, *5*, 743.
(4) Hubbard, C. R.; Jacobson, R. A. *Proc. Iowa Acad. Sci.* **1968**, *75*, 85.
(5) Prassides, K.; Day, P.; Cheetham, A. K. *J. Am. Chem. Soc.* **1983**, *105*, 3366.
(6) Day, P. *Inorg. Chem.* **1963**, *2*, 452.
(7) Brauer, G.; Schnell, W. D. *Z. Anorg. Allg. Chem.* **1956**, *283*, 49.
(8) Hewat, A. W., personal communication.
(9) Rae-Smith, A. R.; Cheetham, A. K.; Skarnulis, A. J. *J. Appl. Crystallogr.* **1979**, *12*, 485.
(10) Rietveld, H. M. *J. Appl. Crystallogr.* **1969**, *2*, 65.
(11) Bacon, G. E. "Neutron Diffraction"; Oxford University Press: London, 1975.
(12) Hewat, A. W. *Acta Crystallogr., Sect. A* **1979**, *A35*, 248.

0020-1669/85/1324-0545$01.50/0

Table I. Final Parameters Derived from the Rietveld Refinements of $A_2M^{III}_{0.5}Sb^{V}_{0.5}Cl_6$[a] at 4.7 K with Esd's in Parentheses (Space Group $Fm3m$; Origin at Center $m3m$)

A	Rb	Rb	Rb	Rb	Cs	Cs
M^{III}	Rh^{III}	Fe^{III}	In^{III}	Tl^{III}	Fe^{III}	In^{III}
u_{Cl}/a	0.238 30 (11)	0.239 15 (11)	0.241 83 (12)	0.243 30 (17)	0.233 80 (8)	0.237 23 (9)
$B_A/Å^2$	4.38 (10)	3.64 (9)	3.71 (9)	3.47 (8)	2.77 (8)	3.44 (10)
$B_{Cl}/Å^2$	1.01 (3)	0.34 (3)	0.85 (3)	0.84 (3)	0.72 (2)	0.92 (2)
$B_{M,Sb}/Å^2$	0.8 (1)	0.40 (8)	0.5 (1)	0.57 (9)	0.89 (7)	1.1 (1)
$a/Å$	9.9093 (1)	9.9437 (1)	10.0307 (1)	10.0613 (1)	10.2044 (1)	10.2788 (2)
$R_{nuc}/\%$	3.50	2.90	2.15	2.99	2.31	4.34
$R_{profile}/\%$	7.73	6.64	5.74	7.45	6.34	9.85
$R_{wp}/\%$	8.66	8.40	7.33	9.26	8.29	11.78
$R_e/\%$	9.74	6.42	8.03	6.39	8.98	9.35

[a] The atoms were refined in the following positions in the unit cell. 8A in (c) ($\bar{4}3m$): $^1/_4$, $^1/_4$, $^1/_4$. 24Cl in (e) ($4mm$): u, 0, 0. 4(M,Sb) in (a) ($m3m$): 0, 0, 0.

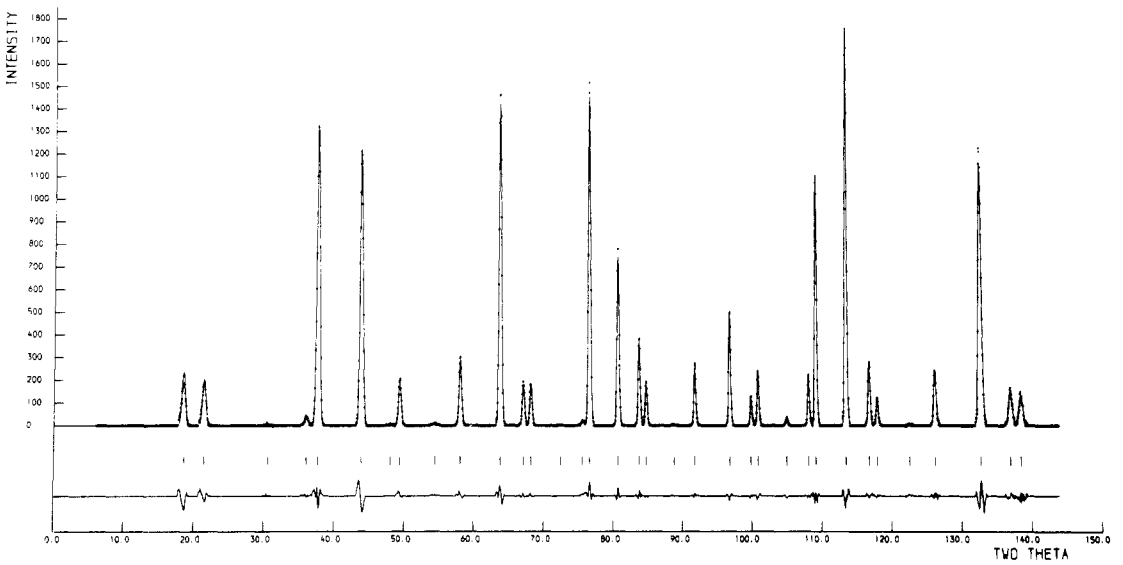

Figure 1. Observed (points), calculated (full curve), and difference profiles for $Cs_2Fe^{III}_{0.5}Sb^{V}_{0.5}Cl_6$ at 4.7 K.

distribution of M^{III} and Sb^V is postulated; i.e., the octahedral sites of the structure are assumed to be occupied by a "hypothetical" ion (M^{III},Sb^V) having a neutron scattering length $\bar{b} = {}^1/_2(b_M + b_{Sb})$. Further, the parameter x that defines the positions of the chlorine atoms in the unit cell gives an average value for the bond lengths M^{III}–Cl and Sb^V–Cl.

With these assumptions, the Rietveld refinements yield the results summarized in Table I. It is noteworthy that the Cs^+ and Rb^+ cations, which occupy the "tetrahedral" holes in the structure, have large, isotropic temperature factors. A typical fit to one of the diffraction profiles of the cubic salts is shown in Figure 1.

Tetragonal Salts. (a) Chlorides. The powder neutron diffraction profiles obtained at 4.7 K for $Cs_2M^{III}_{0.5}Sb^{V}_{0.5}Cl_6$ (M = Bi, Sb, Tl) differ significantly from those of the cubic salts. Weak peaks are clearly visible above the background level, and the main intense peaks decrease in intensity with increasing Bragg angle, θ, being significantly broader than the corresponding reflections in the disordered cubic salts. Further, some peaks clearly show tetragonal splittings that are more pronounced in the order $Cs_2Bi_{0.5}Sb_{0.5}Cl_6$ > $Cs_2Sb^{III}_{0.5}Sb^{V}_{0.5}Cl_6$ > $Cs_2Tl_{0.5}Sb_{0.5}Cl_6$. Since these mixed-valency and mixed-metal salts form solid solutions with antifluorite phases[13] (e.g. $Cs_2Sn^{IV}Cl_6$), and since the main peaks still index on a pseudocubic face-centered unit cell, we conclude that their structure is based upon the K_2PtCl_6 structure and that the distortion arises from the ordering of the different anions present, a superstructure forming in order to accommodate the two valencies present.

The model used in refining the profiles is essentially the same as the one proposed to account for the room-temperature structures of Rb_2SbBr_6[4] and $(NH_4)_2SbBr_6$.[3] A doubling of the pseudocubic antifluorite unit cell along the c direction is assumed (Figure 2). Two K_2PtCl_6 unit cells are placed on top of each other, resulting in a body-centered tetragonal arrangement that preserves the stacking arrangement of the antifluorite structure along the a and

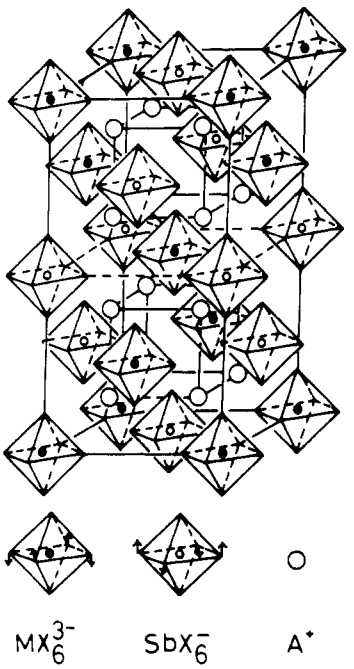

Figure 2. Unit cell of tetragonal $A_2M^{III}_{0.5}Sb^{V}_{0.5}X_6$ compounds.[3] The separate octahedra show the sense of the D_{2d} distortion for two adjacent $M^{III}X_6^{3-}$ and $Sb^VX_6^-$ units along the c axis.

(13) Wells, H. L.; Metzger, F. J. *Am. Chem. J.* **1901**, *26*, 268.

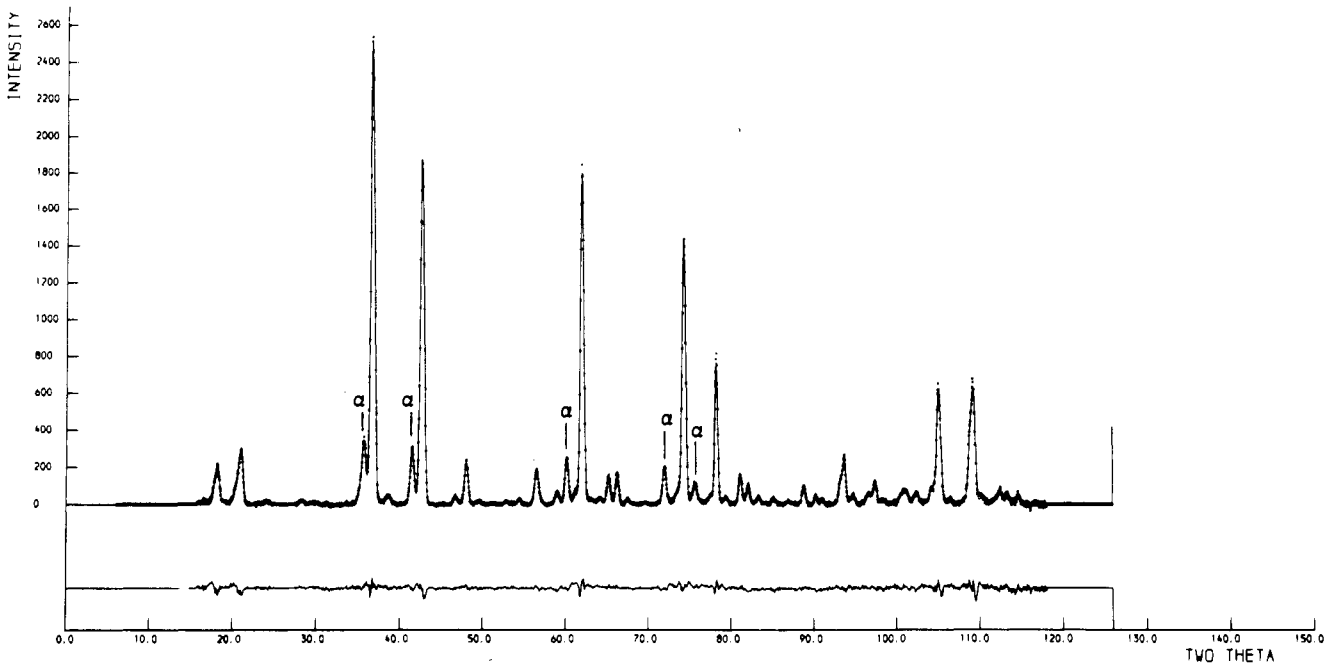

Figure 3. Observed (points), calculated (full curve), and difference profiles for $Cs_2Sb^{III}_{0.5}Sb^{V}_{0.5}Cl_6$ at 298 K. The positions of impurity peak contributions are marked by α.

b crystallographic axes but differs along the *c* axis. Two different oxidation states of the same atom (Sb^{III} and Sb^{V}) or two different atoms (Bi^{III} or Tl^{III} and Sb^{V}) are accommodated, their unequal ionic sizes resulting in c/a ratios differing from 2. The space group $I4_1/amd$ (D^{19}_{4h}) accounts for the extra reflections in the ordered compounds. The origin used in the present refinements is the center of symmetry ($2/m$), at $(0, {}^1/_4, -{}^1/_8)$ from the origin $\bar{4}2m$, used in Figure 2. The MCl_6^{3-} and $SbCl_6^-$ units are not constrained to be octahedral by symmetry as in the K_2PtCl_6 structure. Rather, we can distinguish between two different Cl atoms within each MCl_6^{n-} unit; two equivalent Cl atoms lie along the crystallographic *c* axis (axial) and four (equatorial) have freedom to move parallel to the (010) or (100) planes, providing a route for possible D_{2d} distortions of the MCl_6^{n-} units. The environment of each $SbCl_6^{n-}$ unit is very important in assigning the intermolecular charge-transfer transition

$$Sb^{III}Cl_6^{3-}\ (A) + Sb^{V}Cl_6\ (B) \xrightarrow{h\nu} Sb^{IV}Cl_6^{2-}\ (A) + Sb^{IV}Cl_6^{2-}\ (B)$$

which is responsible for the blue color in Cs_2SbCl_6 and related salts. Each $Sb^{III}Cl_6^{3-}$ ion is surrounded by eight $Sb^{V}Cl_6^-$ units and four $Sb^{III}Cl_6^{3-}$ units, the latter at the corners of a tetrahedron. Initial refinement of the low-temperature Cs_2SbCl_6 structure with 18 independent parameters in $I4_1/amd$ led to the reliability factors $R_p = 0.1505$ and $R_{wp} = 0.1570$. (The Cs_2SbCl_6 profile was originally found to be contaminated by Al peaks resulting from the cryostat. A background cryostat run was also measured and subtracted from the sample run. All Al peaks disappeared except in the region $101.00° < 2\theta < 104.80°$, which was excluded from the refinement.) α-$Cs_3Sb_2Cl_9$ was identified as an impurity, so a multiphase profile analysis program,[14,15] allowing simultaneous refinement of more than one phase contributing to a single profile, was employed for the final refinement of Cs_2SbCl_6. The scale factors for the two phases were constrained to be equal during refinement; the occupation numbers for the seven different atoms in Cs_2SbCl_6 were kept fixed, while the occupation numbers for the five different atoms in α-$Cs_3Sb_2Cl_9$ (space group $P321$[16]) were refined, subject to stoichiometric constraints. This procedure is equivalent to introducing an effective scale factor. Introducing the second phase led to nine extra independent parameters with final reliability factors $R_p = 0.1150$ and $R_{wp} = 0.0920$. The results of the refinement are summarized in Table II, while the observed, calculated, and difference profiles are shown in Figure 3.

Using the single-phase Rietveld refinement technique, we employed the same structural model in the fit of the $Cs_2Bi^{III}_{0.5}Sb^{V}_{0.5}Cl_6$ and $Cs_2Tl^{III}_{0.5}Sb^{V}_{0.5}Cl_6$ profiles at 4.7 K. An absorption correction was applied to the thermal parameters. In these cases, the isotropic temperature factors obtained for the Cs^+ ions are normal (Table II).

Recent far-infrared spectra[17] of Cs_2SbCl_6 were interpreted in terms of increased localization of the Sb^{III} and Sb^{V} oxidation states at low temperatures. In order to study the evolution of the superstructure in the ordered salts $Cs_2M^{III}_{0.5}Sb^{V}_{0.5}Cl_6$ (M = Sb, Bi, Tl), powder neutron diffraction profiles were recorded for these salts at ambient temperature and at 423 K. No changes in the symmetry of the crystals were observed, and for Cs_2SbCl_6 the biphasic refinement technique was again employed. The final results of the refinements are also summarized in Table II. The lattice parameters of α-$Cs_3Sb_2Cl_9$ at 298 K, refined in this way ($a = 7.627$ (2) Å, $c = 9.301$ (1) Å), agree with published X-ray values[16] ($a = 7.633$ Å, $c = 9.345$ Å).

(b) Bromides. The starting model for the refinement of the 4.7 K profile of Rb_2SbBr_6 was $I4_1/amd$, which is the structural model describing its ordered room-temperature structure.[4] This led to unsatisfactory reliability factors ($R_p = 0.1884$ and $R_{wp} = 0.1606$) and highly irregular environments of the two Sb sites. The Sb^{V} ion had four equatorial bromine neighbors at 2.492 Å and two axial at 2.616 Å; the Sb^{III} ion had four bromine neighbors at 2.665 Å and two at 2.803 Å. Use of the biphasic refinement led to no significant improvement so distortion was considered since the K_2PtCl_6 structure is unstable with respect to displacive phase transitions involving tetragonal distortions and/or in-phase (or out-of-phase) rotations of the octahedral MX_6^{2-} units in alternating planes.[18] It is reasonable to postulate a similar phase change for the low-temperature structure of $Rb_2Sb^{III}_{0.5}Sb^{V}_{0.5}Br_6$. The doubling of the pseudocubic K_2PtCl_6 unit cell is again preserved, but to enable the MX_6^{n-} units to rotate, we use the lower symmetry tetragonal space group $I4_1/a$ (C^6_{4h}). Again there are

(14) Thomas, M. W.; Bendall, P. J. *Acta Crystallogr., Sect. A* **1978**, *A34*, S351.
(15) Fitch, A. N.; Wright, A. F.; Fender, B. E. F. *Acta Crystallogr., Sect. B* **1982**, *B38*, 2546.
(16) Kihara, K.; Sudo, T. *Z. Kristallogr.* **1971**, *134*, S142.
(17) Clark, H. W.; Swanson, B. I. *J. Am. Chem. Soc.* **1981**, *103*, 2929.
(18) Sutton, M.; Armstrong, R. L.; Powell, B. M.; Buyers, W. J. L. *Can. J. Phys.* **1981**, *59*, 449.

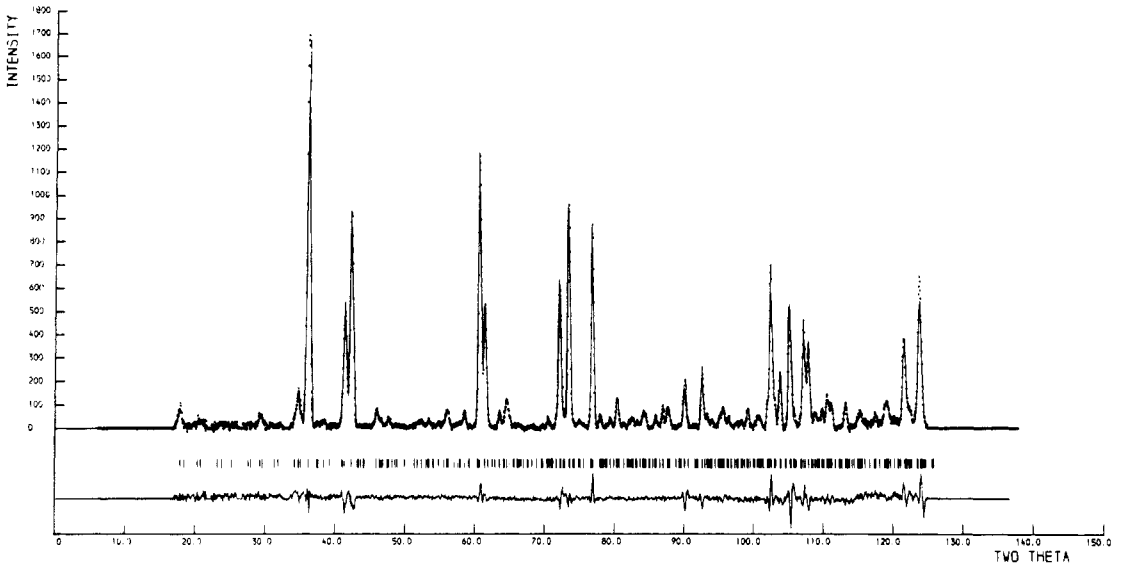

Figure 4. Observed (points), calculated (full curve), and difference profiles for $Rb_2Sb^{III}_{0.5}Sb^{V}_{0.5}Br_6$ at 4.7 K.

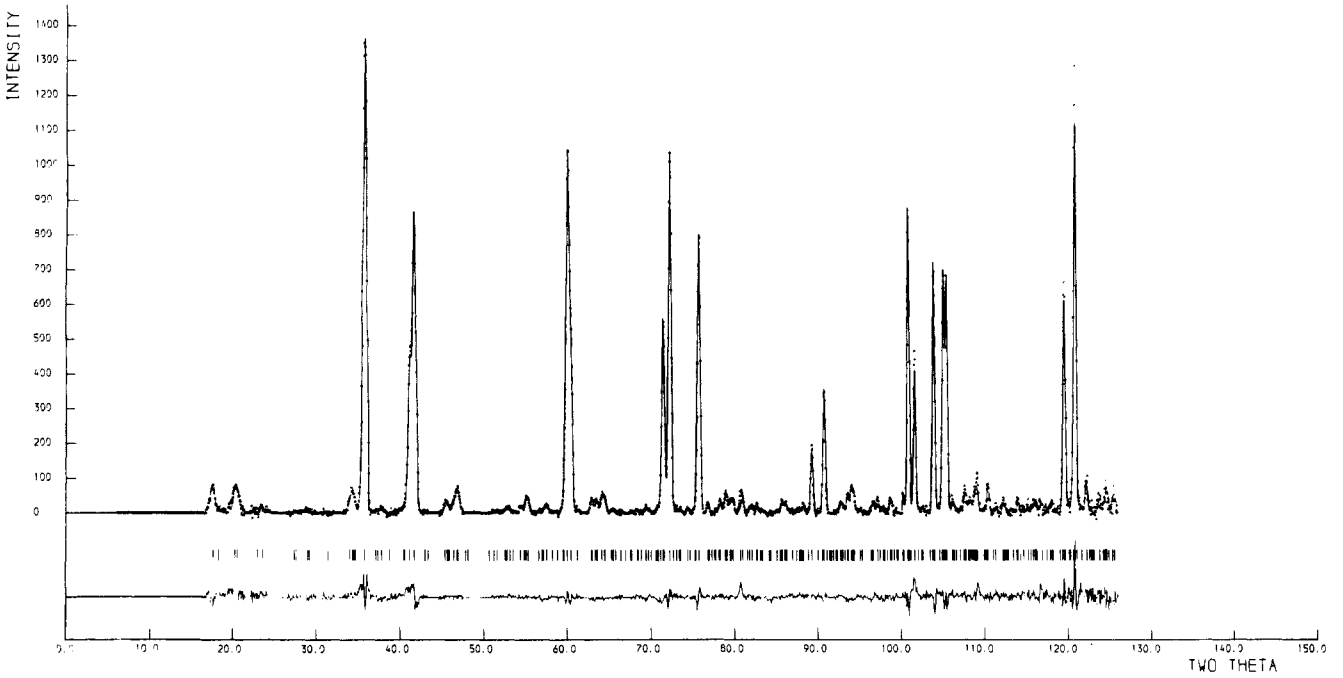

Figure 5. Observed (points), calculated (full curve), and difference profiles for $Cs_2Sb^{III}_{0.5}Sb^{V}_{0.5}Br_6$ at 4.7 K.

two alternative origins; the inversion center $\bar{1}$, which is $(0, -^1/_4, -^1/_8)$ from the origin at $\bar{4}$ (Figure 2), is used in the refinements. The two Sb oxidation states are assigned to positions 4a for Sb^{III} and 4b for Sb^{V}, and the symmetry of the $SbBr_6^{n-}$ units is lowered from D_{2d} to S_4. As in the hexachlorometalates(III,V), two bromine atoms in each $SbBr_6^{n-}$ moiety lie along the crystallographic c axis (axial) occupying the positions 8e, while the four remaining bromine atoms are no longer constrained to lie on the (010) or (100) planes, occupying the general positions 16f and providing a route for rotation of the octahedral Br_6 about the (001) axis. The Rb^+ ions are assigned again to the "tetrahedral" holes, position 16f. The site symmetry of the cation has been reduced from T_d to C_2 to C_1 in going from the $Fm3m$ to the $I4_1/amd$ to the $I4_1/a$ structure. Its position in the hole is not fixed along any crystallographic direction. It still has 12 nearest bromine neighbors, but all Rb–Br distances are different.

Refinement of the profile of Rb_2SbBr_6 in $I4_1/a$ led to the following improved R factors: $R_p = 0.1389$, $R_{wp} = 0.1088$. The $SbBr_6^{3-}$ and $SbBr_6^-$ units rotate about the (001) axis in phase and the Rb^+ ions remain in the tetrahedral hole, moving only marginally along the two new degrees of freedom. The results of the refinement are presented in Table II, while the observed, calculated, and difference profiles are shown in Figure 4.

An attempt was also made to refine the 4.7 K diffraction profile (Figure 5) of $Cs_2Sb^{III}_{0.5}Sb^{V}_{0.5}Br_6$ by using the $I4_1/amd$ structural model, but again the environments of the two Sb oxidation states were highly irregular; Sb(III) formed four bonds of length 2.786 Å and two of 2.593 Å; Sb(V) formed four bonds of length 2.572 Å and two of 2.796 Å. Inspection of the profiles revealed several medium-intensity peaks, well separated from the reflections arising from the $I4_1/amd$ structural model of Cs_2SbBr_6, which could not be assigned as impurities such as $Cs_3Sb_2Br_9$, CsBr, or Al or as arising from the lowering of symmetry of $I4_1/a$. They were therefore excluded from the refinement, which then converged to $R_p = 0.1118$ and $R_{wp} = 0.0853$ (Table II). Reasonable bond lengths and regular environments were then found for the Sb(III) and Sb(V) subunits; i.e., Sb(III) forms four bonds of length 2.776 Å and two of 2.790 Å, and Sb(V) forms bonds of lengths 2.586 and 2.569 Å, respectively. These are in good agreement with the values produced from the Rb_2SbBr_6 refinement at 4.7 K and the ones calculated in the case of room-temperature Rb_2SbBr_6 and $(NH_4)_2SbBr_6$ structures.[3,4] Finally, the c/a ratio of 2.026 com-

Table II. Final Parameters Derived from the Rietveld Refinements of $A_2M^{III}_{0.5}Sb^{V}_{0.5}X_6$[a] (Space Group $I4_1/amd$; Origin at Center (2/m)) and $Rb_2Sb^{III}_{0.5}Sb^{V}_{0.5}Br_6$[b,c] (Space Group $I4_1/a$; Origin at $\bar{1}$) with Esd's in Parentheses

T/K	4.7	298	423	4.7	298	4.7	298	423	4.7	4.7
A	Cs[d]	Cs[d]	Cs	Cs	Cs	Cs	Cs	Cs	Cs	Rb
M	Sb	Sb	Sb	Bi	Bi	Tl	Tl	Tl	Sb	Sb
X	Cl	Cl	Cl	Cl	Cl	Cl	Cl	Cl	Br	Br
x_A	0.2290 (9)	0.2215 (6)	0.2191 (8)	0.2312 (5)	0.2239 (7)	0.2224 (7)	0.2197 (7)	0.2144 (6)	0.2736 (4)	0.2248 (5)
$y_{X(1)}$	0.4810 (4)	0.4804 (4)	0.4788 (6)	0.4829 (3)	0.4798 (4)	0.4844 (4)	0.4814 (5)	0.4806 (7)	0.4908 (4)	0.4905 (5)
$z_{X(1)}$	0.3755 (3)	0.3762 (2)	0.3763 (3)	0.3763 (2)	0.3754 (2)	0.3761 (2)	0.3764 (2)	0.3752 (3)	0.3705 (2)	0.6234 (4)
$y_{X(2)}$	0.5066 (6)	0.5032 (5)	0.5020 (7)	0.5093 (3)	0.5059 (5)	0.4992 (5)	0.4961 (6)	0.4931 (7)	0.5087 (4)	0.5125 (5)
$z_{X(2)}$	−0.1301 (2)	−0.1307 (2)	−0.1310 (3)	−0.1300 (2)	−0.1307 (2)	−0.1288 (2)	−0.1307 (3)	−0.1302 (3)	−0.1238 (3)	0.1308 (3)
$z_{X(3)}$	0.2598 (4)	0.2627 (3)	0.2639 (4)	0.2612 (2)	0.2621 (3)	0.2615 (4)	0.2626 (4)	0.2620 (5)	0.2569 (2)	0.5068 (3)
$z_{X(4)}$	0.0026 (4)	−0.0001 (3)	−0.0014 (4)	0.0032 (3)	0.0009 (3)	−0.0023 (3)	−0.0024 (4)	−0.0039 (6)	−0.0033 (3)	0.2549 (3)
B_A/Å^2	0.4 (1)	1.8 (1)	2.8 (2)	1.49 (9)[e]	2.3 (1)	0.3 (1)[e]	1.7 (1)	1.8 (2)	0.1 (1)[e]	0.2 (1)[e]
B_X/Å^2	0.37 (3)	3.04 (3)	4.50 (4)	1.22 (3)[e]	3.35 (4)	0.66 (2)[e]	2.64 (4)	4.21 (5)	0.25 (3)[e]	0.40 (4)[e]
B_M/Å^2	0.1 (1)	1.47 (9)	2.2 (1)	0.7 (2)[e]	1.7 (1)	0.75 (6)[e]	1.96 (9)	2.9 (1)	0.23 (8)[e]	0.6 (1)[e]
a/Å	10.3092 (3)	10.4650 (2)	10.5400 (4)	10.3558 (2)	10.4928 (2)	10.2994 (4)	10.4271 (3)	10.4963 (3)	10.7320 (1)	10.5487 (1)
c/Å	20.7288 (7)	21.0095 (7)	21.1556 (11)	20.8415 (6)	21.1017 (6)	20.6114 (15)	20.8866 (11)	21.0346 (15)	21.7442 (2)	21.5586 (4)
R_n/%	9.24	5.58	10.90	5.13	5.25	6.95	7.28	8.18	7.06	8.72
R_p/%	11.50	9.47	12.17	9.93	10.24	11.80	12.78	14.81	11.18	13.89
R_{wp}/%	9.20	6.58	8.24	9.15	8.39	11.40	9.92	11.13	8.53	10.88
R_e/%	6.11	5.63	7.20	5.17	6.30	4.70	5.79	6.51	6.42	6.50

[a] The atoms were refined in the following positions in the unit cell. 16A in (f) (2): x, 1/2, 0. 16X(1), 16X(2) in (h) (m): 0, y, z. 8X(3), 8X(4), in (e) (mm): 0, 1/4, z. 4Sb in (b) ($\bar{4}2m$): 0, 1/4, 3/8. 4M in (a) ($\bar{4}2m$): 0, 1/4, −1/8. [b] The atoms were refined in the following positions in the unit cell. 16A, 16X(1), 16X(2) in (f) (1): x, y, z. 8X(3), 8X(4) in (e) (2): 0, 1/4, z. 4Sb in (b) ($\bar{4}$): 0, 1/4, 5/8. 4M in (a) ($\bar{4}$): 0, 1/4, 1/8. [c] Additional positional parameters: $y_A = 0.4983$ (14), $z_A = 0.0032$ (4), $x_{X(1)} = 0.0243$ (5), $x_{X(2)} = 0.0131$ (5). [d] Biphasic refinement. [e] Absorption correction applied.

pared very well with those of the rest of the bromides having an $I4_1/amd$ structure (see Table IV).

The final parameters derived from the refinement, after the application of an absorption correction in the usual way, are presented in Table II.

Discussion

Structural Details and Trends. Some interatomic distances and angles and their estimated standard deviations for the ordered hexahalide salts are summarized in Table III. One important feature of the $I4_1/amd$ space group is that the sites occupied by M(III) and Sb(V) are of D_{2d} symmetry rather than O_h symmetry. From Table III, it can be seen that the (s^0) $Sb^{V}Cl_6^-$ ions show a very small D_{2d} distortion in all salts investigated ($Cs_2M^{III}_{0.5}Sb^{V}_{0.5}Cl_6$; M = Sb, Bi, Tl) at all temperatures. The average Cl_{eq}–Sb(V)–Cl_{ax} is 90.5° in these compounds. In contrast, both the two s^2 ionic complexes $SbCl_6^{3-}$ and $BiCl_6^{3-}$ and the s^0 $TlCl_6^{3-}$ ion show larger distortions. In the case of the $SbCl_6^{3-}$ ion, the distortion is 2.3 (1)° at 4.7 K increasing to 2.7 (1)° at 423 K; with $BiCl_6^{3-}$ it increases from 2.2 (1)° at 4.7 K to 2.6 (1)° at 298 K, and with $TlCl_6^{3-}$ it increases from 1.7 (1)° at 4.7 K to 2.5 (1)° at 423 K. The distortions in neighboring MCl_6^{3-} and $SbCl_6^-$ subunits on the (001) plane are in opposite directions.

Small distortions from perfect octahedral symmetry are not surprising in view of crystal-packing considerations. What is worth commenting on is the lack of even greater distortion for the s^2 ionic complexes $BiCl_6^{3-}$ and $SbCl_6^{3-}$. According to the valence-shell electron-repulsion theory, $SbCl_6^{3-}$ and $BiCl_6^{3-}$ should possess a stereochemically active electron pair, leading to highly distorted octahedra, possibly approaching seven-coordination. However, the distortions of the octahedra determined in this work and for other hexahalide complexes of Se(IV) or Te(IV) are very small. The other notable feature is the reluctance of s^2 ions like Sb(III) to enter into distinct octahedral coordination. For example, while $CsSb^{V}Cl_6$ is a very favored phase thermodynamically, Sb^{III} forms $Cs_3Sb_2Cl_9$ in preference to $Cs_3Sb^{III}Cl_6$; in this way the s^2 "inert" pair plays a structural role since in $Cs_3Sb_2Cl_9$ distinct $SbCl_3$ units are present with a clear lone-pair position. It is only in ionic lattices where strong crystal forces are present that Sb(III) is forced to form discrete octahedral $SbCl_6^{3-}$ units. Such cases are $[Co(NH_3)_6^{3+}][SbCl_6^{3-}]$, where $SbCl_6^{3-}$ is virtually undistorted, and presumably $Cs_4[SbCl_6^-][SbCl_6^{3-}]$, where a mere 2.5° D_{2d} distortion exists. It may be because of the strong lattice forces in the antifluorite-based structures that $Sb^{III}Cl_6^{3-}$ and $Sb^{V}Cl_6^-$ are forced to be structurally more similar than would be expected in terms of their electronic structures.

The situation is more irregular if we turn to the mixed-valency hexabromoantimonates(III,V). The X-ray studies[3,4] have shown, surprisingly, that in $(NH_4)_2SbBr_6$ there is a 3.7 (2)° distortion of the $Sb^{V}Br_6^-$ ion while $Sb^{III}Br_6^{3-}$ is virtually undistorted (0.3 (1)°); in contrast, in Rb_2SbBr_6 there are 1.3 (1)° $Sb^{V}Br_6^-$ and 1.2 (1)° $Sb^{III}Br_6^{3-}$ distortions. At low temperatures, there are 0.8 (2)° for $Sb^{V}Br_6^-$ and 2.6 (1)° S_4 distortions for $Sb^{III}Br_6^{3-}$ in Rb_2SbBr_6 (Table III); in contrast, in Cs_2SbBr_6 there exists a 2.2 (1)° D_{2d} distortion for $Sb^{V}Br_6^-$, while $Sb^{III}Br_6^{3-}$ is almost undistorted (0.5 (1)°). This situation is difficult to rationalize. A clear conclusion is that the $Sb^{V}Br_6^-$ octahedra distort more easily than the $Sb^{V}Cl_6^-$ units. An explanation can be afforded by using an ionic model argument. A cation will be stable in an octahedral hole in a lattice of closest-packed anions if it is at least large enough to keep the anions from touching, i.e. $r_+/r_- > 0.414$. The effective ionic radius ratio for the $Sb^{V}Cl_6^-$ unit is $r(Sb^{5+})/r(Cl^-) = 0.443$, while for the $Sb^{V}Br_6^-$ unit $r(Sb^{5+})/r(Br^-) = 0.407$. Thus, on a purely ionic basis the size of the octahedral hole in the bromides is too large to accommodate the Sb(V) cation, and anion inter-electronic repulsions are minimized by distortion of the octahedral unit.

Within each MX_6^{n-} moiety, the van der Waals contacts between the halogen ions vary because of the distortion from octahedral symmetry; the larger the M–X bond lengths, the larger the van der Waals contacts are. In the case of the $Sb^{V}Cl_6^-$ unit, the mean van der Waals contact is 3.38 Å, while in the case of the trivalent

Table III. Some Bond Distances (Å) and Angles (deg) for the SbX_6^- and MX_6^{3-} Moieties in the Ordered $A_2M^{III}_{0.5}Sb^V_{0.5}X_6$ Compounds

T/K	A	M^{III}	X	Sb^V–X_{ax}	Sb^V–X_{eq}	M^{III}–X_{ax}	M^{III}–X_{eq}	X_{eq}–Sb^V–X_{ax}	X_{eq}–M^{III}–X_{ax}
4.7	Cs	Sb	Cl	2.389 (7)	2.381 (3)	2.645 (9)	2.647 (7)	90.3 (1)	87.7 (1)
298				2.360 (7)	2.411 (4)	2.624 (7)	2.652 (6)	90.6 (1)	87.4 (1)
423				2.351 (9)	2.412 (6)	2.615 (10)	2.660 (7)	90.6 (2)	87.2 (1)
4.7	Cs	Bi	Cl	2.371 (5)	2.412 (3)	2.673 (5)	2.688 (3)	90.65 (7)	87.78 (7)
298				2.382 (6)	2.411 (5)	2.657 (6)	2.688 (5)	90.21 (11)	87.42 (8)
4.7	Cs	Tl	Cl	2.339 (7)	2.414 (5)	2.529 (6)	2.567 (5)	90.5 (1)	88.3 (1)
298				2.348 (9)	2.413 (6)	2.561 (9)	2.569 (7)	90.7 (1)	87.3 (1)
423				2.376 (12)	2.420 (8)	2.547 (13)	2.555 (8)	90.1 (2)	87.5 (1)
4.7[a]	Rb	Sb	Br	2.549 (7)	2.550 (6)	2.800 (8)	2.776 (6)	90.8 (2)	87.4 (1)
298[b]				2.640 (8)	2.553 (5)	2.713 (4)	2.787 (4)	91.3 (1)	88.8 (1)
4.7	Cs	Sb	Br	2.569 (5)	2.586 (5)	2.790 (6)	2.776 (4)	92.2 (1)	89.5 (1)
298[c]	NH_4	Sb	Br	2.559 (5)	2.566 (6)	2.794 (5)	2.795 (6)	93.7 (2)	89.7 (1)

[a] $\theta[001] = 5.77\ (11)^\circ$ and $2.85\ (11)^\circ$ for $Sb^VBr_6^-$ and $Sb^{III}Br_6^{3-}$, respectively. [b] Reference 4. [c] Reference 3.

Table IV. Correlation between Superlattice Tetragonal Distortion and Average Bond Lengths (Å) of MX_6^{n-} Units in $A_2M^{III}_{0.5}Sb^V_{0.5}X_6$[a]

T/K	A	M^{III}	X	space group	av M^{III}–X	av Sb^V–X	$M^{III,V}$–X	c/a
298	Cs	Sb	Br					2.024[b]
4.7		Sb		$I4_1/amd$	2.779 (7)	2.580 (9)	2.680 (8)	2.026
298	Rb	Sb		$I4_1/amd$	2.763 (37)	2.550 (47)	2.657 (42)	2.026[b,c]
4.7		Sb		$I4_1/a$	2.781 (13)	2.550 (6)	2.666 (9)	2.044
298	NH_4	Sb		$I4_1/amd$	2.792 (4)	2.552 (10)	2.672 (7)	2.019[b,d]
298	Cs	Bi	Cl	$I4_1/amd$	2.680 (16)	2.404 (15)	2.542 (15)	2.011
4.7		Bi		$I4_1/amd$	2.686 (8)	2.406 (23)	2.546 (15)	2.013
423		Sb		$I4_1/amd$	2.651 (24)	2.401 (33)	2.526 (28)	2.007
298		Sb		$I4_1/amd$	2.644 (14)	2.404 (28)	2.524 (21)	2.008
4.7		Sb		$I4_1/amd$	2.647 (1)	2.382 (5)	2.515 (3)	2.011
423		Tl		$I4_1/amd$	2.554 (5)	2.412 (24)	2.483 (14)	2.004
298		Tl		$I4_1/amd$	2.567 (4)	2.401 (35)	2.484 (19)	2.003
4.7		Tl		$I4_1/amd$	2.557 (20)	2.399 (40)	2.478 (30)	2.001
4.7		In		$Fm3m$			2.438 (1)	
4.7		Fe		$Fm3m$			2.386 (1)	
4.7	Rb	Tl		$Fm3m$			2.448 (2)	
4.7		In		$Fm3m$			2.426 (1)	
4.7		Fe		$Fm3m$			2.378 (1)	
4.7		Rh		$Fm3m$			2.361 (1)	

[a] The expressions $\bar{x} = \Sigma_{i=1}^{n}(x_i/s_i^2)/\Sigma_{i=1}^{n}(1/s_i^2)$ and $s(\bar{x}) = [\Sigma_{i=1}^{n}(x_i - \bar{x})^2/(n-1)]^{1/2}$ were used to estimate average bond lengths and standard errors; x_i, individual bond lengths; s_i, the associated standard deviations; n, the number of bond lengths. [b] Reference 28. [c] Reference 4. [d] Reference 3.

cations it increases from approximately 3.62 Å for Tl(III) to 3.74 Å for Sb(III) to 3.79 Å for Bi(III). Similarly, in the case of the $Sb^VBr_6^-$ unit, the mean van der Waals contact for the bromine atoms is 3.63 Å, while for $Sb^{III}Br_6^{3-}$ it is 3.94 Å. Furthermore, electron transfer should certainly take place between adjacent $Sb^{III}X_6^{3-}$ and $Sb^VX_6^-$, but in all cases the halogen–halogen contacts between the two units are clearly larger than the sums of their van der Waals radii. In the case of Cs_2SbCl_6 these chlorine–chlorine distances increase, because of thermal expansion, from an average value of 3.73 Å at 4.7 K to 3.83 Å at 298 K to 3.88 Å at 423 K, to be compared with 3.5 Å for their sum of van der Waals radii. Similarly, in the case of Cs_2SbBr_6 the bromine–bromine contact between neighboring units of different valency is 3.84 Å, while in the case of Rb_2SbBr_6 it is 3.74 Å for the Br···Br sum.

Ordered and Disordered Compounds. To identify why some of the M^{III},Sb^V compounds are ordered and some are disordered, we note from Table IV that the average (M^{III},Sb^V)–X bond lengths span a range from 2.680 Å (Cs_2SbBr_6, 4.7 K) to 2.361 Å ($Rb_2Rh_{0.5}Sb_{0.5}Cl_6$). The change from order to disorder occurs between 2.478 Å ($Cs_2Tl_{0.5}Sb_{0.5}Cl_6$) and 2.448 Å ($Rb_2Tl_{0.5}Sb_{0.5}Cl_6$). Hence, it appears that salts with an average (M^{III},Sb^V)–X bond length greater than 2.478 Å are ordered while all those where it is less than 2.448 Å are disordered. Since the Sb^V–X bond lengths are essentially constant, the difference in size between $M^{III}X_6^{3-}$ and $Sb^VX_6^-$ appears to be the controlling factor. When the MX_6 ions are close in size, no superlattice ordering is observed, even in salts such as $A_2Fe_{0.5}Sb_{0.5}Cl_6$ (A = Rb, Cs) in which the difference in neutron scattering lengths is larger (i.e. $b_{Sb} = 0.56 \times 10^{-12}$ cm, $b_{Fe} = 0.96 \times 10^{-12}$ cm) for ions that may occupy different sites in the structure. In contrast, superlattice peaks are observed even in cases like $A_2Sb^{III}_{0.5}Sb^V_{0.5}X_6$ where the ions of different oxidation states have the same neutron scattering length.

Furthermore, Table IV shows that the magnitude of the tetragonal distortion, as measured by the c/a ratio, follows the same trend. Thus, the larger the difference in size between the SbX_6^- and MX_6^{3-} units, the larger the tetragonal distortion. The only discrepancy occurs with Rb_2SbBr_6 at 4.7 K, which shows a larger c/a ratio (2.044) than expected, no doubt because of the rotation of the octahedral units and the accompanying phase transition. Otherwise, Cs_2SbBr_6 with an average (Sb^V,Sb^{III})–Br bond length of 2.680 Å shows the largest tetragonal distortion ($c/a = 2.026$), while $Cs_2Tl_{0.5}Sb_{0.5}Cl_6$ with an average (Sb^V,Tl^{III})–Cl bond length of 2.478 shows the smallest ($c/a = 2.001$).

At this point, we note that the bond length around the ions of different oxidation states,[19] is an important parameter in theories of electron transfer in mixed-valency compounds. It is proportional to the electron–phonon coupling constant measuring the horizontal displacement in vibrational coordinate space of the potential energy surfaces describing the ground and excited states. Certainly in mixed-valency hexahalogenoantimonates(III,V), such differences in bond lengths are surprisingly small in view of the localized character of the compounds and the nonexistence of the Sb(IV) state (see ref 20 for a quantitative discussion of this point). In the present case, we find the average Sb^V–Cl bond to be 2.401 Å, while Sb^{III}–Cl is 2.647 Å; similarly Sb^V–Br is 2.558 Å and Sb^{III}–Br is 2.779 Å. Metal–chlorine distances for the disordered cubic compounds can only be estimated indirectly. Adopting a constant value for the Sb^V–Cl bond distances equal to 2.401 Å,

(19) Prassides, K.; Day, P. *J. Chem. Soc., Faraday Trans. 2* **1984**, *80*, 85.
(20) Prassides, K.; Day, P. *Inorg. Chem.*, in press.

we can estimate the following bond lengths: In^{III}–Cl = 2.475 Å in $Cs_2In_{0.5}Sb_{0.5}Cl_6$ and 2.451 Å in $Rb_2In_{0.5}Sb_{0.5}Cl_6$; Fe^{III}–Cl = 2.371 Å in $Cs_2Fe_{0.5}Sb_{0.5}Cl_6$ and 2.355 Å in the $Rb_2Fe_{0.5}Sb_{0.5}Cl_6$; Tl^{III}–Cl = 2.495 Å in $Rb_2Tl_{0.5}Sb_{0.5}Cl_6$ (cf. the observed Tl^{III}–Cl in the Cs salts of 2.557 Å); Rh^{III}–Cl = 2.321 Å in $Rb_2Rh_{0.5}Sb_{0.5}Cl_6$.

An electrostatic calculation[21] shows that any ordered structure of the hexahalogenoantimonates(III,V) and related salts that increases the number of the M^{III},Sb^V neighbors at the expense of M^{III},M^{III} and Sb^V,Sb^V near neighbors increases the lattice energy compared to the disordered structure where the M^{III} and Sb^V units are statistically distributed over the lattice sites. Thus to explain the occurrence of the large number of disordered structures in this group of compounds, kinetic reasons must be invoked for the absence of a phase transition to the ordered superstructure. The apparent isotropic *B* factors (Table I) of the cations occupying the "tetrahedral" holes in the disordered compounds are larger than expected on thermal grounds alone. Applying the absorption correction[12] may lead to overestimated *B* values, but they may also reflect static displacements around the mean position of the cations as a result of the small differences in their environments.

The hexahalogeno complexes of tetravelent metal ions of the type $A_2M^{IV}X_6$ (A = K^+, NH_4^+, Rb^+, Cs^+; X = Cl, Br, I) have been extensively studied in the last few years since many of them undergo one or several phase transitions as the temperature is lowered.[22,23] At high temperatures, most complexes possess the antifluorite K_2PtCl_6-type structure in space group $Fm3m$. In general, on lowering the temperature, they undergo structural phase transitions to tetragonal and eventually monoclinic structural arrangements, most of which are linked with the softening of rotary phonons and the hindered rotation of the MX_6^{2-} octahedra.[24] The phase-transition temperatures[19] decrease with increasing size of the cations that occupy the "tetrahedral" holes in the structure and with decreasing size of the halogen ligand. In the series of mixed-valency and mixed-metal salts, the crystal lattice is based on the K_2PtCl_6 structure, and between 4.7 and 423 K, there is no phase transition resulting from mutual rotation of the pseudooctahedral MCl_6^{3-} and $SbCl_6^-$ units in the lattice for the compounds Cs_2SbCl_6, $Cs_2Tl_{0.5}Sb_{0.5}Cl_6$, and $Cs_2Bi_{0.5}Sb_{0.5}Cl_6$. At all temperatures, the axial Cl atoms are aligned along the same axis and the equatorial Cl atoms lie on the same plane, the structure being always $I4_1/amd$. The only variation is due to thermal expansion resulting in a volume increase for all three salts of ca. 0.04% from 4.7 K to room temperature. Further, there is no significant change in the c/a ratio. Even at 4.7 K Cs_2SbBr_2, too, shows no evidence of mutual rotation of the $SbBr_6^{3-}$ and $SbBr_6^-$. However, in Rb_2SbBr_6, with the smaller Rb^+ cation and the larger, more polarizable Br ligands, a phase transition occurs between room temperature and 4.7 K as a result of which the $Sb^VBr_6^-$ and $Sb^{III}Br_6^{3-}$ octahedra rotate around the (001) axis (Figure 6), i.e. a ferrorotative transition. The angle of rotation of the $SbBr_6^-$ ions from their equilibrium position with respect to the *c* crystal axis is 5.8°, while the corresponding angle for the $SbBr_6^{3-}$ ions is 2.8° (Table III). The volume change between 4.7 K and room temperature is again ca. 0.04%; this shows that there is negligible volume change accompanying the phase transition. However, the c/a ratio for the low-temperature phase of Rb_2SbBr_6 is no longer in line with the tetragonal distortions observed for the other compounds; its value is 2.044 to be compared with that of 2.026 at room temperature. Hence, the ferrorotative transition is accompanied by a further elongation of the unit cell along the *c* axis. The primitive unit cell however remains the same. From this discussion, we can conclude that the structural change seems to occur as a result of the softening of the symmetric combination of the rotary phonon modes of the $SbBr_6^-$ and $SbBr_6^{3-}$ ions in the primitive unit cell at the Γ point of the Brillouin zone.

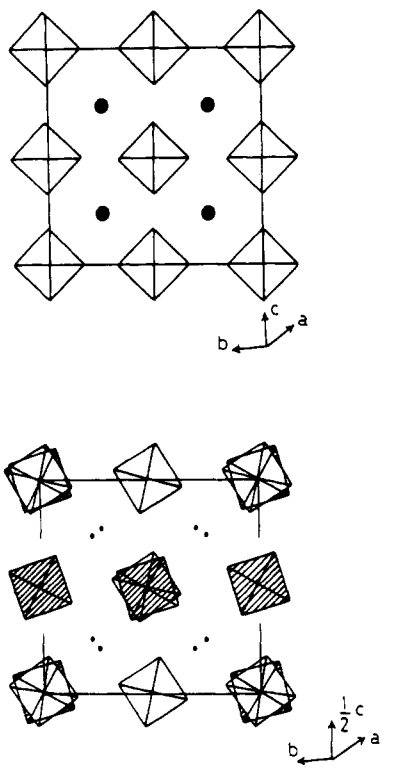

Figure 6. Projections of the unit cells of K_2PtCl_6 (upper) and $Rb_2Sb^{III}_{0.5}Sb^V_{0.5}Br_6$ (lower) on the *ab* plane. Shaded squares describe the $Sb_VBr_6^-$ ion; unshaded ones, the $Sb^{III}Br_6^{3-}$ units.

Vibrational Spectra of Hexachloroantimonates(III,V). Infrared and Raman spectra have been used to confirm the existence of distinguishable $SbCl_6^-$ and $SbCl_6^{3-}$ in Cs_2SbCl_6 (Robin–Day class II).

If we ignore the superlattice of $SbCl_6^{3-}$ and $SbCl_6^-$ and the resulting tetragonal distortion, we can attempt to understand the infrared and Raman spectra of Cs_2SbCl_6 in terms of the zone-center vibrational modes predicted in the $Fm3m$ space group. The primitive unit cell in K_2PtCl_6-type compounds contains nine atoms, and thus there are 27 photon branches in the vibrational spectrum. In the case of Cs_2SbCl_6, there are four active internal infrared modes of symmetry T_{1u}, two from each $SbCl_6^{3-}$ and $SbCl_6^-$ octahedron. The first reported infrared spectrum of Cs_2SbCl_6 showed only two absorptions: a sharp one at 346 cm^{-1}, assigned to $\nu_3(Sb^VCl_6^-)$, and a broad one at 190 cm^{-1}, assigned to $\nu_4(Sb^VCl_6^-)$. The missing $Sb^{III}Cl_6^{3-}$ internal vibrations were contained under the envelope of the latter absorption. In a similar fashion, the resonance Raman spectrum[26] was found to be dominated by bands arising from the $Sb^VCl_6^-$ ion, with only one band due to the $Sb^{III}Cl_6^{3-}$ ion observed (ν_1). A progression in $\nu_1(Sb^VCl_6^-)$ involving a lattice mode at ca. 60 cm^{-1} was observed, indicating that lattice modes participate in the electron-transfer process. A small distortion must be present in the lattice since the formally Raman-forbidden $\nu_3(Sb^VCl_6^-)$ mode appears weakly in the spectrum.

In a recent comprehensive study[17] of the Fourier transform infrared spectra of Cs_2SbCl_6 between 77 and 373 K, a breakdown in mutual exclusion was observed and formally gerade modes ($\nu_1(Sb^V)$, $\nu_2(Sb^V)$, and $\nu_5(Sb^V)$ and $\nu_1(Sb^{III})$ and $\nu_5(Sb^{III})$) are observed in the infrared spectrum. Further, this breakdown is temperature dependent, with the "forbidden" peaks disappearing as the temperature is raised. At 373 K, even the ν_3 and ν_4 ($Sb^{III}Cl_6^{3-}$) modes disappear and the spectrum is a replica of the

(21) Atkinson, L. D.Phil. Thesis, Oxford University, 1967.
(22) Rössler, K.; Winter, J. *Chem. Phys. Lett.* **1977**, *46*, 56.
(23) Van Driel, H. M.; Wiszniewska, M.; Moores, B. M.; Armstrong, R. L. *Phys. Rev. B: Solid State* **1972**, *6*, 1596.
(24) O'Leary, G. P.; Wheeler, R. G. *Phys. Rev. B: Solid State* **1970**, *1*, 4909.
(25) Barrowcliffe, T.; Beattie, I. R.; Day, P.; Livingstone, K. *J. Chem. Soc. A.* **1967**, 1810.
(26) Clark, R. J. H.; Trumble, W. R. *J. Chem. Soc., Dalton Trans.* **1976**, 1145.

infrared spectrum reported by Barrowcliffe et al.[25] Further, formally forbidden modes appear in the infrared spectrum of $Cs_2In^{III}_{0.5}Sb^{V}_{0.5}Cl_6$, but in this case their intensity is independent of temperature.[17] It was postulated that the space group of both compounds is lower than $Fm3m$ and that Cs_2SbCl_6 might undergo a phase change as the temperature is lowered resulting in increased localization of the two Sb valencies in the crystal, in contrast to the mixed-metal In^{III},Sb^{V} salt which shows no evidence of such a transition.

We have found that Cs_2SbCl_6 shows superlattice ordering of $SbCl_6^{3-}$ and $SbCl_6^-$ and the space group is $I4_1/amd$. Sb^{III} and Sb^{V} occupy sites of symmetry D_{2d}, no longer possessing a center of inversion. Taking into account the descent in symmetry from an O_h site to a D_{2d} site, we find that ν_2 and ν_5 should become infrared active. Indeed, $\nu_2{}^{V}$, $\nu_5{}^{V}$, and $\nu_5{}^{III}$ are observed in the infrared spectrum of Cs_2SbCl_6. The appearance of $\nu_1{}^{V}$ and $\nu_1{}^{III}$ cannot be explained by using the site-group symmetry properties. Further, ν_3 and ν_4 become Raman active and this might explain the appearance of $\nu_3{}^{V}$ in the resonance Raman spectrum.

In the primitive unit cell of Cs_2SbCl_6, there are two $Sb^{III}Cl_6^{3-}$ and two $Sb^{V}Cl_6^-$ ions, the full factor-group symmetry being D_{4h}, which possesses a center of inversion. The symmetries of the vibrational modes at the zone center involving the $Sb^{III}Cl_6^{3-}$ and $Sb^{V}Cl_6^-$ units can be obtained by the method of ascent in symmetry[27] whereby a representation of a subgroup (i.e. D_{2d}) can be correlated with those representations of the supergroup (i.e. D_{4h}) that are obtained as ascent in symmetry. However, even allowing for the full factor-group symmetry, it is not possible to account for the appearance of $\nu_1{}^{III}$ and $\nu_1{}^{V}$ in the infrared spectrum of Cs_2SbCl_6.

We have also studied the evolution of the structure of $Cs_2M^{III}_{0.5}Sb^{V}_{0.5}Cl_6$ (M = Sb, Bi, Tl) with temperature. No evidence of a phase transition is apparent between 5 and 423 K. The structure is tetragonal at all temperatures, and the only effect present is that of thermal expansion (approximately isotropic). The tetragonal distortion measured by the c/a ratio is effectively constant as are the D_{2d} distortions of the individual $Sb^{V}Cl_6^-$ and $Sb^{III}Cl_6^{3-}$ ions. Hence the change in intensity of the "forbidden" peaks in the infrared spectrum does not seem to arise from a corresponding evolution of the crystal structure. It is worth noticing that similar "forbidden" peaks, though temperature independent, appear in the infrared spectrum of $Cs_2In^{III}_{0.5}Sb^{V}_{0.5}Cl_6$, whose structure is strictly cubic at low temperatures. The $Sb^{V}Cl_6^-$ and $In^{III}Cl_6^{3-}$ ions are constrained by symmetry to be octahedral in this case. Thus it seems more plausible that the origin of these "forbidden" peaks may lie in the involement of vibrational modes away from the Brillouin zone center.[17] Such phonon dispersion may result in the breakdown of the selection rules. Further, the different temperature behavior of the $InCl_6^{3-}$ and $SbCl_6^{3-}$ ions should certainly arise from the different force fields in these ions. Sb^{III} (s^2) contains an "inert" pair of electrons with the result that the forces within the $SbCl_6^{3-}$ ions do not follow the same trends as other MX_6^{n-} units.

Acknowledgment. We thank Dr. A. Hewat, S. Heathman, and Dr. A. Fitch for their help and the Institut Laue-Langevin for providing neutron beam time. K.P. thanks Christ Church, Oxford, for a Senior Scholarship.

Registry No. $Cs_2Sb^{III}_{0.5}Sb^{V}_{0.5}Br_6$, 12397-94-3; $Rb_2Sb^{III}_{0.5}Sb^{V}_{0.5}Br_6$, 36594-17-9; $Cs_2Bi^{III}_{0.5}Sb^{V}_{0.5}Cl_6$, 12441-33-7; $Cs_2Sb^{III}_{0.5}Sb^{V}_{0.5}Cl_6$, 17805-64-0; $Cs_2Tl^{III}_{0.5}Sb^{V}_{0.5}Cl_6$, 41875-61-0; $Cs_2In^{III}_{0.5}Sb^{V}_{0.5}Cl_6$, 41875-60-9; $Cs_2Fe^{III}_{0.5}Sb^{V}_{0.5}Cl_6$, 61269-02-1; $Rb_2Tl^{III}_{0.5}Sb^{V}_{0.5}Cl_6$, 12432-76-7; $Rb_2In^{III}_{0.5}Sb^{V}_{0.5}Cl_6$, 85370-04-3; $Rb_2Fe^{III}_{0.5}Sb^{V}_{0.5}Cl_6$, 61269-01-0; $Rb_2Rh^{III}_{0.5}Sb^{V}_{0.5}Cl_6$, 85370-05-4.

(27) Boyle, L. L. *Acta Crystallogr., Sect. A* **1972**, *A28*, 172.
(28) Tovborg-Jensen, A.; Rasmussen, S. E. *Acta Chem. Scand.* **1955**, *9*, 708.

Contribution from the Department of Chemistry and Chemical Physics Program, Washington State University, Pullman, Washington 99164-4620

Spectroscopic Assignments of the Excited States of *trans*-$(N_2)_2M(Ph_2PCH_2CH_2PPh_2)_2$ (M = W, Mo)

J. G. BRUMMER and G. A. CROSBY*

Received May 14, 1984

Photoluminescence data on the title compound (M = W) in the temperature range of 1.7–300 K have been analyzed in terms of a manifold of emitting levels in thermal equilibrium. A proposed energy level scheme places a $^3B_{1u}$ (W → phosphorus) charge-transfer term lowest followed by a $^3B_{2g}$ ligand field term ~200 cm^{-1} higher in energy. The latter is assumed to be the precursor level(s) for photochemical dissociation of dinitrogen. The orbital scheme (D_{4h}) e_g (d_{xz}, d_{yz}) < b_{2g} (d_{xy}) << a_{2u} (phosphorus d orbitals) < a_{1g} (d_{z^2}) is proposed for the W(0) complex. For the analogous Mo(0) species, the emission data require an inversion of the highest two orbitals placing a_{1g} (d_{z^2}) lower, a scheme that is consistent with the increased photolability of N_2 in the Mo(0) molecule relative to the W(0) analogue.

Introduction

During the past 15 years a number of studies have appeared on the synthesis,[1] thermal reactivity,[2] and photoreactivity[3-5] of *trans*-$(N_2)_2M(dppe)_2$ [M = Mo(0), W(0); dppe = $Ph_2PCH_2CH_2PPh_2$]. Nitrogen dissociation is now known to be

(1) (a) George, T. A.; Seibold, C. D. *Inorg. Chem.* **1973**, *12*, 2544. (b) George, T. A.; Seibold, C. D. *J. Organomet. Chem.* **1971**, *C13*, 30. (c) Hidai, M.; Tominari, K.; Uchida, Y.; Misona, A. *Inorg. Synth.* **1974**, *15*, 25. (d) George, T. A.; Noble, M. E. *Inorg. Chem.* **1978**, *17*, 1678. (e) Dilworth, J. R.; Richards, R. L. *Inorg. Synth.* **1980**, *20*, 119.
(2) (a) Chatt, J.; Heath, G. A.; Leigh, G. J. *J. Chem. Soc., Chem. Commun.* **1972**, 444. (b) Chatt, J.; Heath, G. A.; Richards, R. L. *J. Chem. Soc., Dalton Trans.* **1974**, 2074. (c) Chatt, J.; Pearman, A. J.; Richards, R. L.; *Nature (London)* **1975**, *253*, 39. (d) Chatt, J.; Diamantis, A. A.; Heath, G. A.; Hooper, N. E.; Leigh, G. J. *J. Chem. Soc., Dalton Trans.* **1977**, 1688. (e) Colquhoun, H. M. *Acc. Chem. Res.* **1984**, *17*, 23 and references therein.
(3) (a) George, T. A.; Iske, S. D. A. "Proceedings of the First International Symposium on Nitrogen Fixation"; Newton, W. E., Nyman, N. J., Eds.; Washington State University: Pullman, WA, 1976; p 27. (b) Chatt, J.; Diamantis, A. A.; Heath, G. A.; Leigh, G. J.; Richards, R. L. "Proceedings of the First International Symposium on Nitrogen Fixation"; Newton, W. E.; Nyman, N. J., Eds.; Washington State University: Pullman, WA, 1976; p 17. (c) Day, V. W.; George, T. A.; Iske, S. D. A. *J. Am. Chem. Soc.* **1975**, *97*, 4127. (d) Chatt, J.; Pearman, A. J.; Richards, R. L. *J. Chem. Soc., Dalton Trans.* **1977**, 1852. (e) Caruana, A.; Hermann, H.; Kisch, H. *J. Organomet. Chem.* **1980**, *187*, 349.
(4) Chatt, J.; Head, R. A.; Leigh, G. J.; Pickett, J. *J. Chem. Soc., Dalton Trans.* **1978**, 1638.

0020-1669/85/1324-0552$01.50/0